CFD analysis of concept car in order to improve aerodynamics

DARKO DAMJANOVIĆ
DRAŽAN KOZAK
MARIJA ŽIVIĆ
ŽELJKO IVANDIĆ
TOMISLAV BAŠKARIĆ
Mechanical Engineering Faculty in Slavonski Brod, Josip Juraj Strossmayer University of Osijek, Croatia

Car is designed using the software package Autodesk 3ds Max. Polygonal modeling method was used and the designed car represents a new conceptual solution of car design. After modeling a car with the mentioned software, final digital images are generated too. Final digital images are generated using the Mental Ray rendering tool as a default rendering tool of Autodesk 3ds Max. Attention is given only to the external design of the car, while the interior is not modeled. Furthermore, using the software ANSYS Fluent, 2D simulation of the airflow around the side contour of the vehicle was made in the purpose of making changes in the geometry of the vehicle to improve the design in terms of reducing air resistance and improving aerodynamics. Most attention is given to changing value of angle between the hood and front windshield of the car, and analysing the back of the car with and without the rear wing. Leading to the obtained 2D simulation and leading with modifications of the initial 2D model, an existing 3D car model is redesigned. According to our assumption, new 3D car model has better aerodynamic properties. The 3D analysis of the redesigned car model in terms of mentioned changes is performed too in order to analyse possible improvements compared to the initial design.

1 INTRODUCTION

The importance of aerodynamics can be seen from a simple example: If we need to raise the top speed of Ferrari Testarossa from 180 mph (≈289 km/h) to 200 mph (≈321 km/h) like Lamborghini Diablo, and without altering its shape, we need to raise its engine power from 390 hp to 535 hp. Besides, another approach is to analyse geometry in wind tunnel and making CFD analysis to decrease its Cd (Drag Coefficient) from 0.36 to 0.29, and with that we can do the same thing [1].

2 CAR 3D MODEL AND RENDERINGS

The car model is madewith the software Autodesk 3ds Max. Polygonal modeling method was used for creating the car geometry. The final model with all details consists of 507 984 polygons and 568 254 vertexes. The polygonal model is presented in **Figure 1.**

3 COMPUTATIONAL FLUID DYNAMICS (CFD)

There are two possibilities to analyse the aerodynamic features of vehicles and especially the turbulences: the wind tunnel and computational fluid dynamics (CFD). The efficiency and the financial aspect make CFD a better solution. Even the visualization and the accuracy are other aspects which show the advantages of CFD.

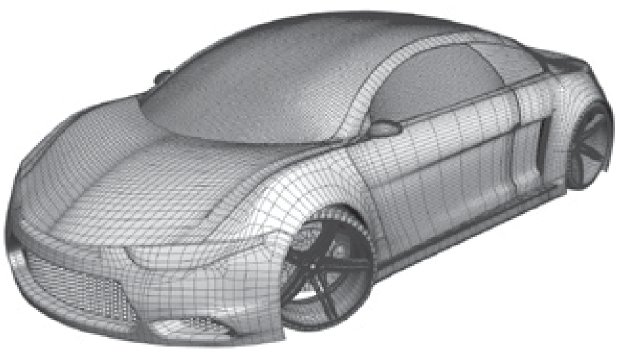

Figure 1: Polygonal car model

New turbulence models and the increasing computing power make CFD much more important [2].

Finite volume method (FVM) was used in CFD analysis of airflow around a car. For 2D analysis of the airflow around the side contour of a car, the software GAMBIT was used as preprocessor for modeling and discretization of the problem, and the software FLUENT was used as solver and postprocessor. For 3D analysis of the airflow around the car geometry, the software ANSYS CFX was used.

3.1 Theory

The governing equations for computational fluid dynamics are based on conservation of mass, momentum and energy. Both FLUENT and ANSYS CFX use a FVM to solve the governing equations. The FVM involves discretization and integration of the governing equations over the finite volume [4].

The flow is said to be turbulent when all the transport quantities (mass, momentum and energy) exhibit periodic, irregular fluctuations in time and space. Such conditions enhance mixing of these transport variables. There is no single turbulent model that can resolve the physics at all flow conditions. FLUENT and ANSYS CFX provides a wide variety of models to suit the demands of individual classes of problems. The choice of the turbulent model depends on the required level of accuracy, the available computational resources and the required turnaround time [5].

For the problem analysed in this paper, standard κ - ε turbulent model is selected for both 2D and 3D analysis. The κ - ε model is one of the most common turbulent models. It is a semi - empirical, two-equation model, which means, it includes two extra transport equations to represent the turbulent properties of the flow. The first transport variable is the turbulent kinetic energy κ. The second transport variable is the turbulent dissipation ε. It is the variable that determines the scale of the turbulence, whereas the first variable k determines the energy in the turbulence.

The model transport equation for k is derived from the exact equation, while the model transport equation for κ is obtained using physical reasoning and bears little resemblance to its mathematically exact counterpart [5].

3.1.1 Governing equations

The continuity and momentum equations (Navier - Stokes equations) with a turbulence model were used to solve the airflow [9]:

$$\frac{\partial u}{\partial x}+\frac{\partial v}{\partial y}+\frac{\partial w}{\partial z}=0, \tag{1}$$

$$u\frac{\partial u}{\partial x}+v\frac{\partial u}{\partial y}+w\frac{\partial u}{\partial z}=-\frac{1}{\rho}\frac{\partial p}{\partial x}+\frac{1}{\rho}\left(\frac{\partial \tau_{xy}}{\partial y}+\frac{\partial \tau_{xz}}{\partial z}\right)+B_x \ , \tag{2}$$

$$u\frac{\partial v}{\partial x}+v\frac{\partial v}{\partial y}+w\frac{\partial v}{\partial z}=-\frac{1}{\rho}\frac{\partial p}{\partial y}+\frac{1}{\rho}\left(\frac{\partial \tau_{xy}}{\partial x}+\frac{\partial \tau_{yz}}{\partial z}\right)+B_y \ , \tag{3}$$

$$u\frac{\partial w}{\partial x}+v\frac{\partial w}{\partial y}+w\frac{\partial w}{\partial z}=-\frac{1}{\rho}\frac{\partial p}{\partial z}+\frac{1}{\rho}\left(\frac{\partial \tau_{xz}}{\partial x}+\frac{\partial \tau_{yz}}{\partial y}\right)+B_z \ . \tag{4}$$

Where u is x - component of velocity vector, v is y - component of velocity vector and w is z - component of velocity vector. ρ is density of air, p is static pressure, τ is shear stress and B_x, B_y, B_z are body forces [9].

3.1.2 Transport equations for standard κ - ε turbulent model

- for turbulent kinetic energy k:

$$\frac{\partial}{\partial t}(\rho k)+\frac{\partial}{\partial x_i}(\rho k u_i)=\frac{\partial}{\partial x_j}\left[\left(\mu+\frac{\mu_t}{\sigma_k}\right)\frac{\partial k}{\partial x_j}\right]+G_k+G_b-\rho\,\varepsilon-Y_M+S_k \tag{5}$$

-for dissipation ε:

$$\frac{\partial}{\partial t}(\rho\,\varepsilon)+\frac{\partial}{\partial x_i}(\rho\,\varepsilon u_i)=\frac{\partial}{\partial x_j}\left[\left(\mu+\frac{\mu_t}{\sigma_\varepsilon}\right)\frac{\partial \varepsilon}{\partial x_j}\right]+C_{1\varepsilon}\frac{\varepsilon}{k}(G_k+C_{3\varepsilon}G_b)-C_{2\varepsilon}\rho\frac{\varepsilon^2}{k}+S_\varepsilon \tag{6}$$

In these equations, G_k represents the generation of turbulence kinetic energy due to the mean velocity gradients. G_b is the generation of turbulence kinetic energy due to buoyancy. Y_M represents the contribution of the fluctuating dilatation in compressible turbulence to the overall dissipation rate. C_{1e}, C_{2e} and C_{3e} are constants. σ_k and σ_ε are the turbulent Prandtl numbers for κ and ε, respectively. S_k and S_e are user-defined source terms [5].

3.1.3 Turbulent viscosity

$$\mu_t=\rho C_\mu\frac{k^2}{\varepsilon} \tag{7}$$

where C_μ is constant [5].

3.1.4 Production of turbulent kinetic energy

From the exact equation for the transport of k, this term may be defined as:

$$G_k=-\rho\,\overline{u_i'u_j'}\frac{\partial u_j}{\partial x_i} \tag{8}$$

To evaluate G_k in a manner consistent with the Boussinesq hypothesis:

$$G_k=\mu_t S^2, \tag{9}$$

where S is the modulus of the mean rate - of - strain tensor, defined as:

$$S\equiv\sqrt{2S_{ij}S_{ij}}, \tag{10}$$

$$\text{where}\quad S_{ij}=\frac{1}{2}\left(\frac{\partial u_i}{\partial u_j}+\frac{\partial u_j}{\partial u_i}\right)\quad [5]. \tag{11}$$

3.1.5 The generation of turbulence due to buoyancy

$$G_b=\beta g_i\frac{\mu_t}{\mathrm{Pr}_t}\frac{\partial T}{\partial x_i}, \tag{12}$$

where Pr_t is the turbulent Prandtl number for energy and gi is the component of the gravitational vector in the i - th direction. For the standard and realizable models, the default value of Pr_t is 0.85 [4].

The coefficient of thermal expansion β is defined as:

$$\beta=-\frac{1}{\rho}\left(\frac{\partial p}{\partial T}\right)_p \quad [5]. \tag{13}$$

3.1.6 The dilatation dissipation

The dilatation dissipation term Y_M, is included in the k equation. This term is modeled according to:

$$Y_M=2\rho\,\varepsilon M_t^2 \tag{14}$$

where M_t^2 is the turbulent mach number, defined as:

$$M_t=\sqrt{\frac{k}{a^2}} \tag{15}$$

where a is the speed of sound:

$$a\equiv\sqrt{\gamma RT}\quad [5]. \tag{16}$$

3.1.7 Model constants

The model constants C_{1e}, C_{2e}, C_μ, σ_k and σ_e have the following default values:

$C_{1e}=1.44,\ C_{2e}=1.92,\ C_\mu=0.09,\ \sigma_k=1.0,\ \sigma_e=1.3.$

These default values have been determined from experiments with air and water for fundamental turbulent shear flows including homogeneous shear flows and decaying isotropic grid turbulence. They have been found to work fairly well for a wide range of wall - bounded and free shear flows [5].

4 TWO-DIMENSIONAL CFD ANALYSIS OF SIDE CONTOUR OF THE CAR

2D analysis are very helpful and usually preceded by a 3D analysis, because they can provide some basic guidelines that could be redesigned on the product in order that the resulting 3D analysis provide better and more acceptable results. This approach can significantly shorten the time of analysing a problem, because the 2D analysis in relation to 3D is of course much simpler and the time for obtaining a solution is much shorter. So, the 2D analysis is a good indicator of the real state, however it is necessary to note that the results could significantly change when the same problem is considered in 3D.

4.1 Discretization of the 2D domain

After meshing problem in GAMBIT, the mesh consists of quads and triangulars. As **Figures 3** and **4** show, the mesh is discretized

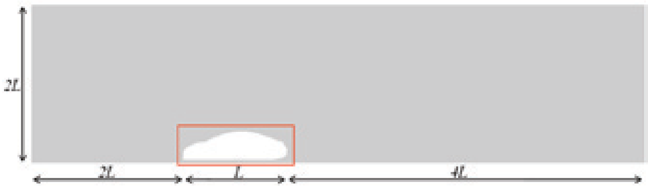

Figure 2: Dimensions and discretization of 2D domain

4.2 Boundary conditions

Velocity of the air at the inlet boundary condition is set in FLUENT with a value of 27,7 m/s (≈100 km/h) and with a temperature of 300 K (≈26,85°C). The outlet boundary condition is set to pressure outlet with the gauge pressure of 0 Pa. The car contour, the top and the bottom of the virtual wind tunnel are set as walls. The density of air is set as 1.225 kg/m^3 and the viscosity of air is 1.7894 x 10^{-5} kg/(ms).

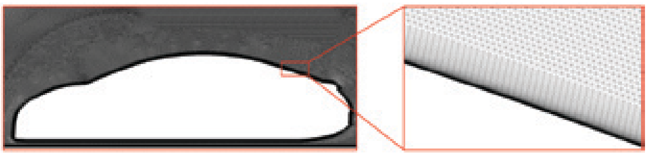

Figure 3: Finite volume mesh of the first case of car geometry (initial car geometry)

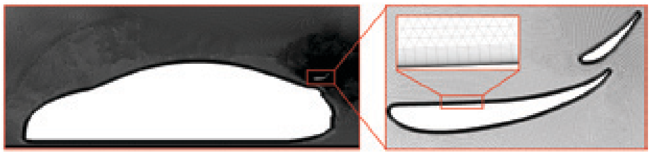

Figure 4: Finite volume mesh of the second case of car geometry (redesigned geometry)

as structured close to the car contour and on the top and the bottom of the domain too. Dimensions of analysis domain are presented in **Figure 2**, where L = 4500 mm.

As mentioned earlier, two cases of car geometry was analysed. The first case is the initial design, so the geometry of the existing model and the second case are redesigned geometry in terms of increasing the angle between the hood and the front windshield to get a better airflow around the car. Also, in the redesigned car geometry, rear wing is added in the purpose to see changes and analyse airflow with the rear wing. **Figure 3** shows the finite volume mesh of the first case of car geometry and **Figure 4** shows the second case of car geometry with the mentioned changes.

4.3 Results

Figure 5 shows the velocity contours of the initial car geometry, and **Figure 6** shows the velocity contours of the redesigned car geometry. Figures show that the air velocity is decreasing as it is approaching the front of the car. Then air velocity increases away from the car front. In the second case, the velocity magnitude increases with a higher gradient, which means that the air resistance is smaller.

Figures 7 and **8** shows static pressure contours. It is obvious from the Figures that there is a higher pressure concentration on the car front in both cases, and at the rear wing in the second case.

Particularly, the air slows down when it approaches the front of the car and results in that more air molecules are accumulated into

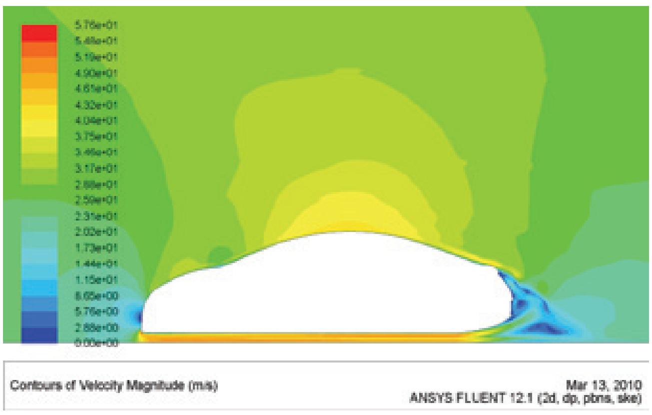

Figure 5: Velocity contours over the initial car geometry (first case)

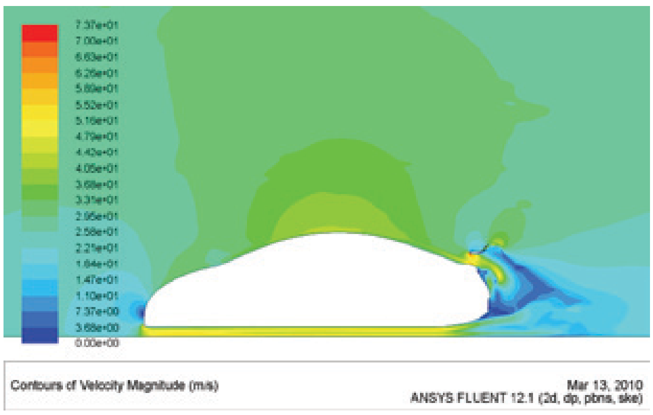

Figure 6: Velocity contours over the redesigned car geometry (second case)

Figure 7: Static pressure contours over the initial car geometry (case one)

Figure 8: Static pressure contours over the redesigned car geometry (case two)

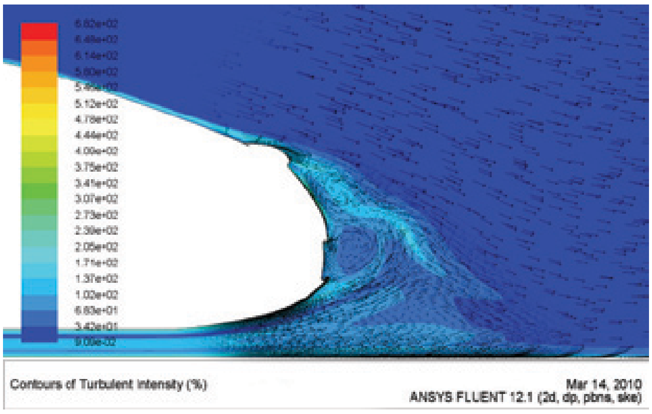

Figure 9: Turbulence intensity contours + vectors over the initial car geometry (first case)

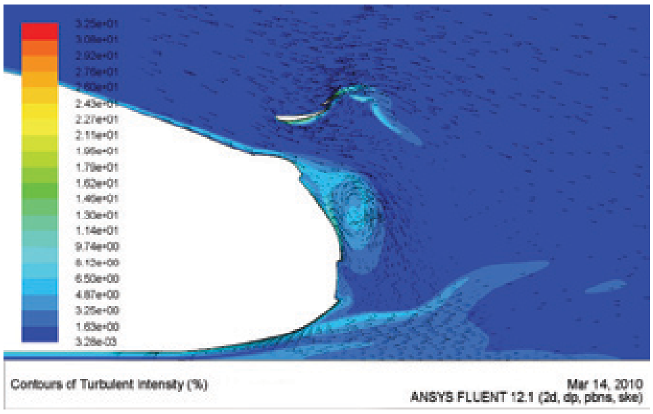

Figure 10: Turbulence intensity contours + vectors over the redesigned car geometry (second case)

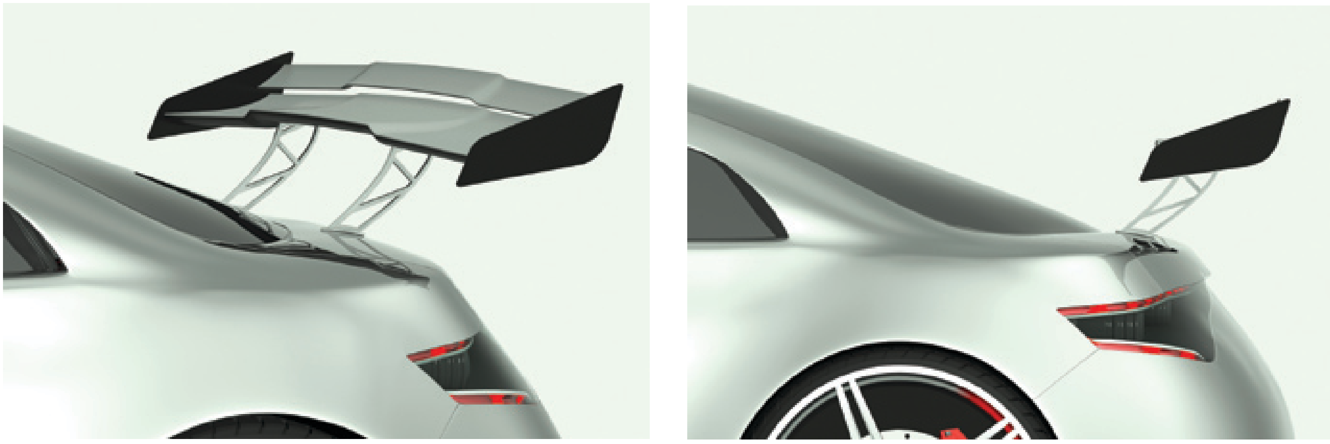

Figure 11: Design of the rear wing

a smaller space. Once the air stagnates in front of the car, it seeks a lower pressure area, such as the sides, top and the bottom of the car. As the air flows over the car hood, pressure is decreasing, but when reaches the front windshield, it increases briefly. When the higher-pressure air in front of the windshield travels over the windshield, it accelerates, causing the decrease of the pressure. This lower pressure literally produces a lift - force on the car roof as the air passes over it [6].

Also, **Figure 8** shows that there is a larger amount of pressure on the top surface of the rear wing. That pressure is generating a bigger down-force resulting in better stability of the car and increasing traction. The wing is a very efficient aerodynamic add-in, because it creates lots of down - force and thereby with small effect to increasing drag.

Figures 9 and **10** show turbulence intensity contours + vectors for both cases of car geometry. It is obvious from the presented Figures that the rear wing has big significance to the turbulences. It can be seen that in case of the redesigned car geometry there is less turbulences behind the car and the turbulent zone is cleaner.

5 REDESIGNED CAR MODEL

Leading to the modifications of an existing model in terms of the redesigned side contour of the car and leading with the obtained 2D results of the airflow around the car, the existing 3D car model has been redesigned. The new model has a slightly larger number of polygons due to the added rear wing. After applying materials and textures to each part of car and scene, each photograph takes about 2,5 hour for rendering. The mental Ray rendering tool was used for rendering as a default rendering tool of Autodesk 3ds Max.

Figure 11 shows the design of the rear wing, and **Figure 12** shows some of the renderings of the new, redesigned car model.

6 THREE DIMENSIONAL CFD ANALYSIS OF CAR

Also in this case, both geometries of The car were analysed. Some details such as car wheels, breaks, exhaust, etc. are disposed from the 3D analysis in the purpose of simplifying the model and the analysis too. However, in spite of the fact of that the model consists of quite number of elements.

6.1 Discretization of the 3D domain

Due to the full symmetry of the problem, only one half of the domain is meshed and after meshing the domain in ANSYS, the mesh consists of 1874264 nodes and 6148164 elements in case of the initial car geometry, and of 2854713 nodes and 9560271 elements in case of the redesigned car geometry. **Figure 13** shows dimensions of the analysis domain, where L = 4500 mm.

The mesh is discretized as structured close to the car contour and on the bottom of domain too. **Figure 14** shows the surface mesh of the full meshed domain, and **Figure 15** shows some surface mesh details of the structured mesh around the car geometry.

As in the case of the 2D analysis, to get the most accurate results and within the most identical conditions, the mesh is discretized in both cases of the geometry with the same density. The

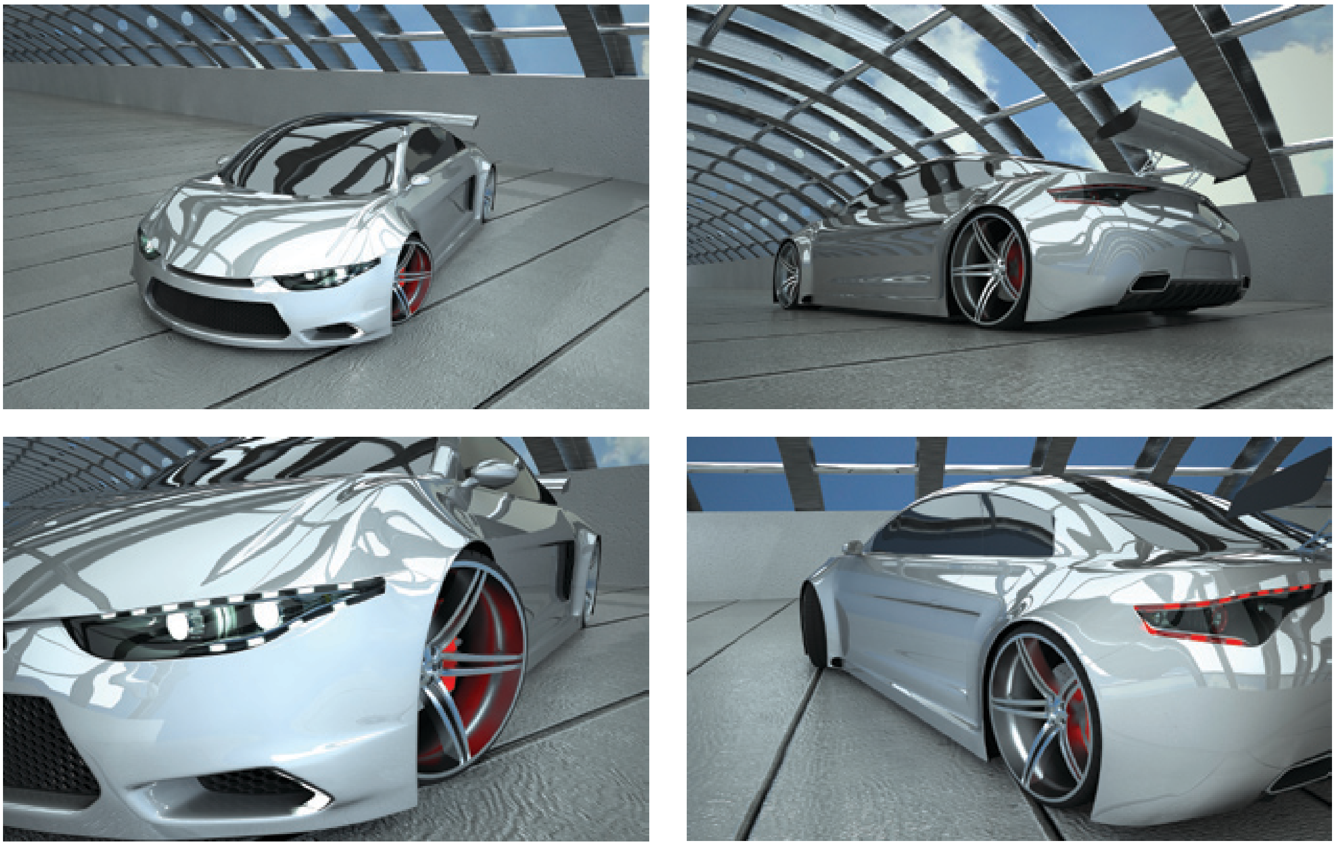

Figure 12: Renderings of the redesigned car model

only difference is that in case of the redesigned car geometry, the mesh has a higher number of elements. That is because the rear wing is added in the redesigned car geometry, and the mesh is generated around it with more density, **Figure 16** and **17**.

Figure 16 and 17 show the volume mesh and some details of the structured volume mesh around the rear wing and the side mirror.

6.2 Boundary conditions

The material is set as "Air Ideal Gas" and the velocity of the air at the inlet boundary condition is set in ANSYS CFX with a value of 27,7 m/s (≈100 km/h) and with a temperature of 300 K (≈26,85°C). The κ - ε turbulent model is selected. The whole car body and the bottom of the virtual wind tunnel are set as smooth wall with the option of "No Slip Wall". The top and the side of the tunnel are set as "Wall" with the option of "Free Slip Wall". The outlet boundary condition is set to "Outlet" with the relative static pressure of 0 Pa. And the "Symmetry" boundary condition is set to the symmetry plane. **Figure 17** shows the boundary conditions of the 3D domain **(Figure 18)**.

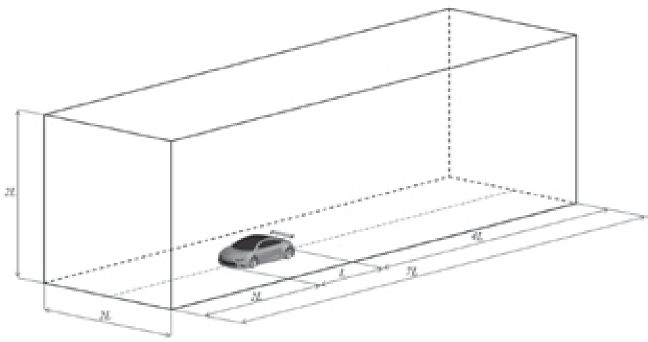

Figure 13: Dimensions of the 3D domain

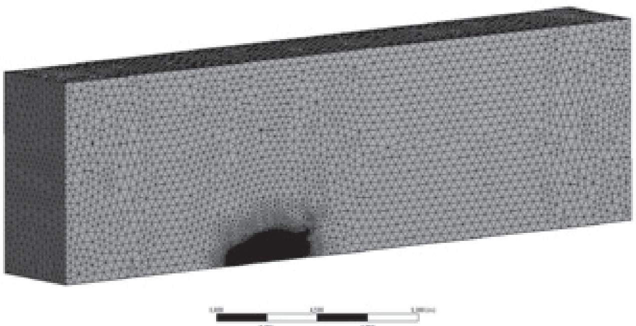

Figure 14: The meshed domain

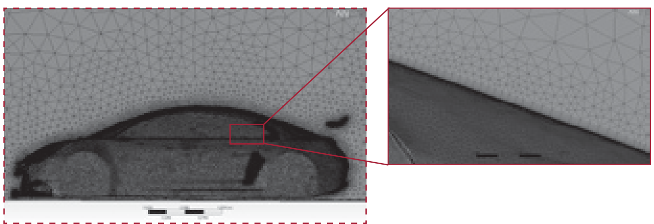

Figure 15: Surface mesh of the domain

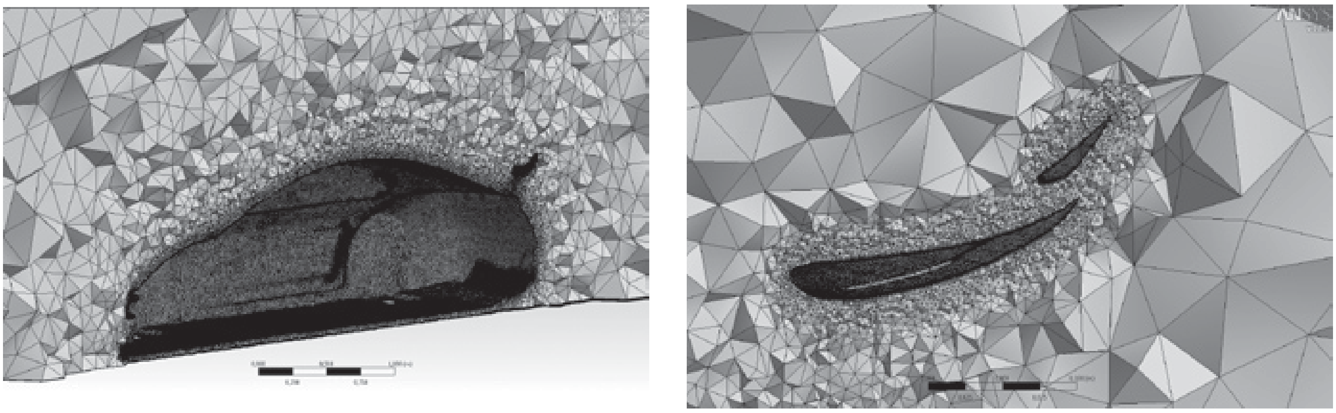

Figure 16: Details of the finite volume mesh around the car geometry

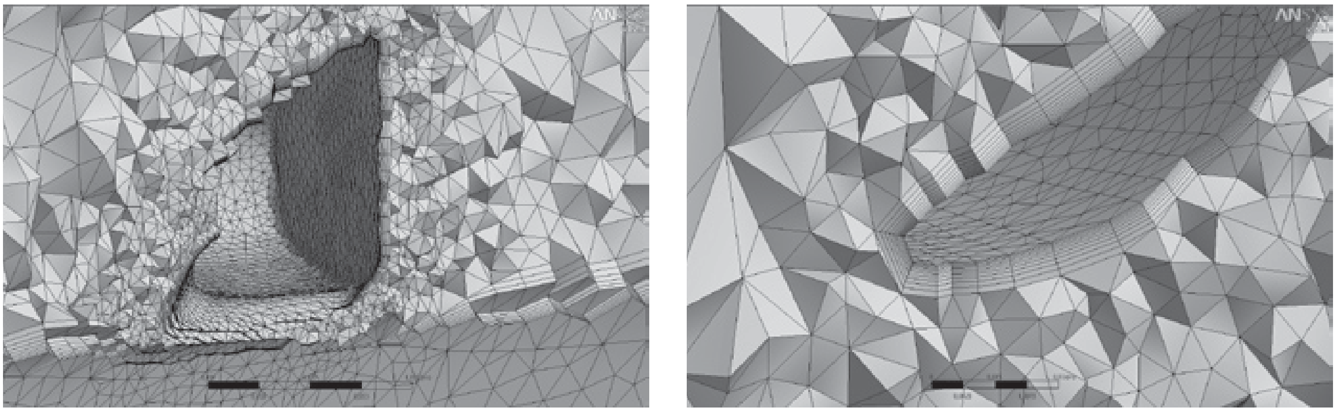

Figure 17: Details of the structured mesh on the side mirror and the rear wing

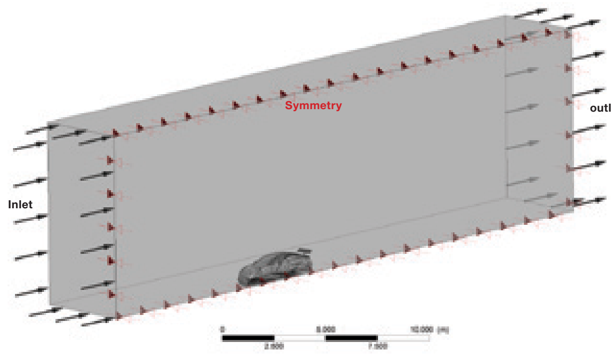

Figure 18: Boundary conditions of the 3D domain

6.3 Results

Unfortunately, due to the lack of computer equipment, the geometry of the car is simplified, and thus the CFD analysis, so among other things, the wheels are ejected from the analysis.

In a further work, the aim is to create a CFD simulation of a car in motion, so with rotating wheels and moving ground. Also in the performed analysis, the entry of the air into the front and the side air intakes are not taken into consideration, which quite changes a realistic picture of the results, so in a further work, our plan is to take that into consideration too.

Figure 19 shows the pressure distribution on 3D model of the car and the ground from front and rear of the car. As expected, from pressure contours it is obvious that there is a larger pressure amount in front of the car, especially at the front and the side air intakes. In case of the redesigned car geometry, the maximum pressure amount is on the top surface of the rear wing, and the result of that is generating a down - force. How wings generate down – force, will be discussed hereafter.

Figures from 20 to 22 shows velocity streamlines over both car geometries, from different angels and for some individual parts of the car.

Figure 22 shows velocity streamlines below the car. As shown in the 2D analysis, once again, it is confirmed that by adding a rear wing on a car, there is less turbulences behind the car. It is also obvious that the velocity streamlines by distancing from the initial car geometry are expanding, while in the opposite situation, in case of a car with rear wing, velocity streamlines are narrowing. This means that the turbulent zone behind the redesigned car is smaller.

More turbulence behind the initial car geometry is also obvious from **Figure 21,** which presents the velocity streamlines on the symmetry plane, so the eddy's are easier to see.

The reason for the expanding of velocity streamlines in the case of geometry without rear wing is that the air after passing over the rear windshield travels directly to the ground. That air has a higher speed and comes into collision behind the car with the air from below the car which has a lower speed. So the expanding of velocity streamlines are caused by distancing from the car. By using the rear wing, the opposite occurs, because the airflow is directing upwards by the rear wing and thus allows slower air from below the car to free flow by distancing from the car, so there is no expanding of the airflow, **Figure 22.**

Figure 23 shows the velocity and the pressure distribution over the rear wing. The rear wings are nearly irrelevant in ordinary passenger cars, but when it comes to sports cars, especially those for race,

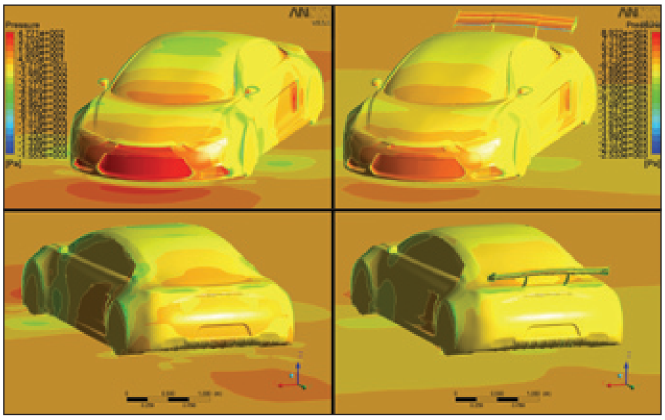

Figure 19: Pressure distribution on the car body and the ground

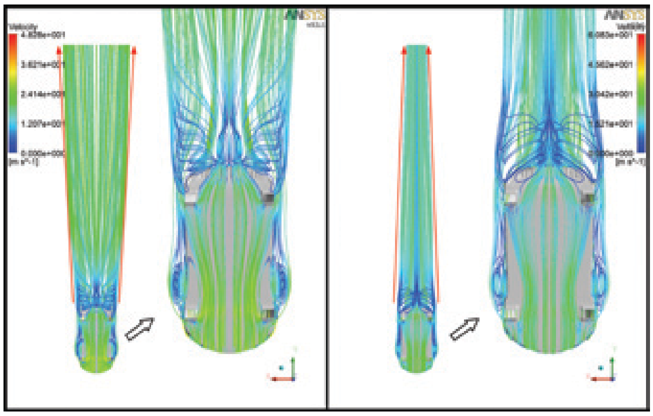

Figure 22: Velocity streamlines from below the car

these are the most important aerodynamic add - ins. For example, for a F1 car, the rear wing creates around a third of the car down - force [7]. But running at high speeds the drag from the rear wing is huge. It would be the best to achieve the following: more down - force at lower speeds in the purpose of increasing traction and thus better acceleration, and less down – force at higher speeds when the car is on a straight line and doesn't need down – force.

A wing generates down - force due to its profile accelerating airflow on its lower surface in relation to the flow over the top surface. If the flow is accelerated, the pressure is decreasing, resulting in a pressure differential between the upper and lower surface of the wing and thus generating a down - force [8].

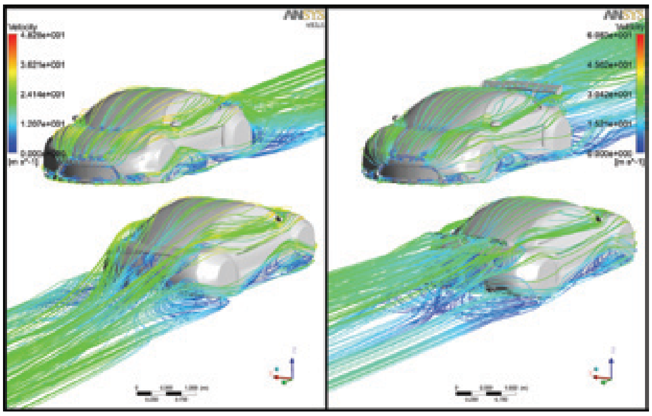

Figure 20: Velocity streamlines over the car body

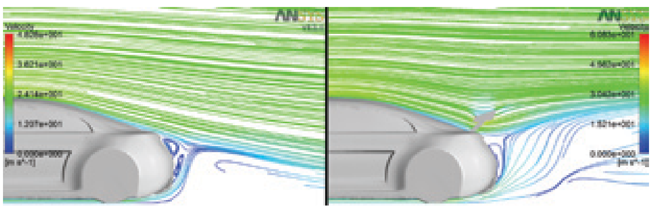

Figure 21: Velocity streamlines on the symmetry plane of the car

As the air flows over the surface of a wing, it has a tendency to slow down and separate from the wing, particularly underneath the wing which runs at a lower pressure than the top surface, **Figure 23.** This separation initially reduces efficiency and the airflow totally breaks up and the wing stalls. When a wing stalls, it loses most of its down - force (that is required at higher speeds) [7]. But at lower speeds, the aim is to prevent separation. So it is needed to speed up the flow near the wing surface [7]. To achieve both, dual element wings are used, **Figure 23**. These allow for some of the high pressure flow from the top surface of the lower wing to bleed to the lower surface of the upper wing. This increases the airflow speed under the wing, increasing down – force and reducing the boundary flow separation [8].

Otherwise, because there is an increased loading that comes with higher speeds on the straight and due to flexi upper wing it will deflect (or just part of it), and thus the upper wing will move closer to the lower wing resulting in the gap between them becoming smaller. This leads to the separation and wing stalls, so that sheds down – force and with that drag.

In order to prove this, the 2D simulation of the airflow around the side contour of the vehicle was made for the velocity of 250 km/h, because the assumption is that at this speed the upper wing will deflect and move closer to the lower wing. **Figure 24** shows that this leads to the separation and the wing stalls.

However, the question is: "How such design of the rear wing affects the aerodynamic drag – force"? Surely, this type of rear wing increases drag – force at higher speeds. So, by different analysis, (CFD and analysis in wind tunnel) it is necessary to find out the compromising solution which will reduce enough down – force at the higher speeds, but of the some time doesn't influence the increase of the drag – force greatly.

7 CONCLUSIONS

On the basis of the car model, 2D and 3D simulations were performed for both car geometries to visualize the airflow and pressure distribution. The mentioned CFD analyses are achieved to see critical places in geometry which are resulting in bad aerodynamics. Leading to the obtained 2D simulation and leading with modifications of an existing 2D model in terms of the redesigned side contour of the car, the existing 3D car model is redesigned. Redesign is in terms of increasing angle between the hood and the front windshield of the car, and adding the rear wing. Furthermore, the 3D analysis of airflow around the redesigned car geometry was achieved. With the obtained 2D and 3D results, it is concluded that the mentioned changes in the geometry of the redesigned car are resulting in better airflow around the car, and producing more down – force using the rear wing. Bigger amount of down – force is resulting in better stability of the car and the increasing traction.

A dual element wing is used because of the possibility to achieve more down – force at lower speeds in the purpose of increasing traction and thus better acceleration and less down – force at higher speeds when car is on a straight line and doesn't need a down – force. Wings are very efficient aerodynamic add – ins, because they create a lot of down – force and thereby with

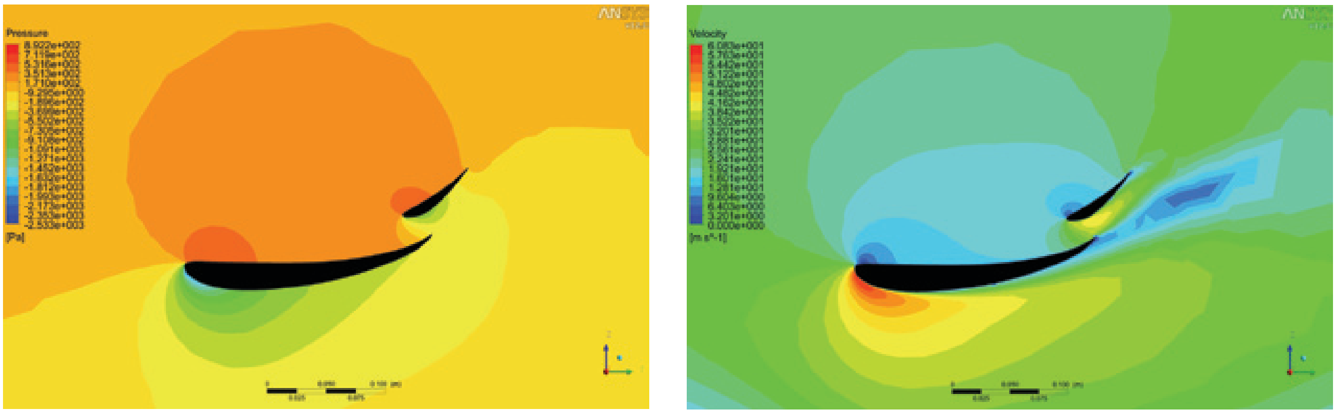

Figure 23: Pressure and velocity contours over the rear wing, deflecting of upper wing

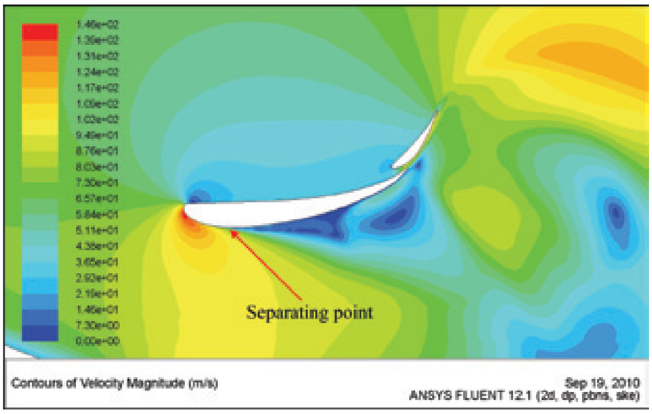

Figure 24: Velocity contours over the rear wing at speed of 250 km/h

small effect on the increasing drag. It is also established that in case of the redesigned car geometry there is less turbulences behind the car and the turbulent zone is cleaner.

Because of the observation that dual-element rear wings are increasing drag - force at higher speeds, it would be necessary to find out the compromising solution which will reduce enough the down – force at the higher speeds, but at the some time doesn't influence the increasing of drag – force greatly.

8 FURTHER WORK

Our aim is to create a CFD simulation of a car in motion, so with rotating wheels and moving ground. Also the entry of air into the front and side air intakes was not take into consideration in these analyses, which quite changes the realistic picture of the results, so in a further work, our plan is to take that into consideration too. With that we will get a more realistic picture of the pressure distribution on the car body and the air flow around the car.

Depending on the capabilities, another plan is the verification of the results obtained with CFD analysis in a way to create a model that will be tested in a wind tunnel.

REFERENCES

[1] http://www.autozine.org/technical_school/aero/tech_aero.htm (17.06.2010)

[2] Milad Mafi, "Investigation of Turbulence Created by Formula One™ Cars with the Aid of Numerical Fluid Dynamics and Optimization of Overtaking Potential", Competence Centre, Transtec AG, Tübingen, Germany

[3] Virag, Zdravko, Lectures from the course "Numerical methods"

[4] Luke Jongebloed, "Numerical Study using FLUENT of the Separation and Reattachment Points for Backwards - Facing Step Flow", Mechanical Engineering Rensselaer Polytechnic Institute, Hartford, Connecticut, December, 2008

[5] ANSYS Fluent, Release 12.1: Help Topics

[6] http://www.up22.com/Aerodynamics.htm (25.07.2010)

[7] http://scarbsf1.wordpress.com/2010/03/04/blown-rear-wings-separating-and-stalling/ (07.09.2010)

[8] http://www.racecar-engineering.com/articles/f1/449813/f-ducts-how-do-they- work.html (08.09.2010)

[9] Popat, B.C., 1991. Study of Flow and Noise Generation from Car A-pillars, Ph.D. Thesis, Department of Aeronautics, Imperial College of Science, Technology and Medicine, The University of London, UK.

AUTHOR DATA

Darko Damjanović, Dražan Kozak, Marija Živić, Željko Ivandić, Tomislav Baškarić

Mechanical Engineering Faculty in Slavonski Brod, Josip Juraj Strossmayer University of Osijek. Trg Ivane Brlić Mažuranić 2, HR-35000 Slavonski Brod, Croatia.

E-mail: darko.damjanovic@gmail.com, dkozak@sfsb.hr, mzivic@sfsb.hr, zivandic@sfsb.hr, tomislav.baskaric@gmail.com.

This paper was presented in a similar form at the International Scientific and Expert Conference TEAM 2010, Kecskemét, November 4-5, 2010 as a plenary/keynote lecture.